

Forward Pion Production in Hadron Collisions at STAR

G. Rakness^a, for the STAR Collaboration

^aPenn State University/Brookhaven National Laboratory,
Physics 510-A, Upton, NY 11973

Measurements are reported of the production of high energy π^0 mesons at large pseudorapidity, coincident with charged hadrons at mid-rapidity, for proton+proton and deuteron+gold collisions at $\sqrt{s_{NN}} = 200$ GeV. The p+p cross section for inclusive π^0 production follows expectations from next-to-leading order perturbative QCD. A suppression of the back-to-back azimuthal correlations was observed in d+Au, qualitatively consistent with the gluon saturation picture. Experimental uncertainties regarding the inclusive measurement are discussed.

1. INTRODUCTION

In contrast to the case for the nucleon, little is known about the distribution of gluons in nuclei, especially in the region of Björken- $x < 0.01$, where x is the fraction of the nucleon's momentum carried by the parton. Studies of deuteron(proton)+nucleus collisions at large center of mass energy ($\sqrt{s_{NN}}=200$ GeV) can provide constraints on the gluon density in heavy nuclei. In the perturbative QCD explanation of particle production at large pseudorapidity, a large- x parton scatters from a low- x parton and then fragments into the observed particle(s). Forward charged particle production is found to be suppressed in d+Au collisions [1], consistent with the expectation of gluon saturation [2,3], possibly indicating a different mechanism for particle production. Explanations of the suppression based on leading-twist pQCD calculations using a model of gluon shadowing have also been suggested [4]. Further tests of the possible role played by gluon saturation at RHIC energies are provided by the study of particle correlations [5,6].

At $\sqrt{s}=200$ GeV and larger collision energies, there is quantitative agreement between NLO pQCD calculations and measured p+p cross sections at mid-rapidity [7]. This agreement has been found to extend to π^0 production at $\langle \eta \rangle = 3.8$ [8]. Further tests of the underlying dynamics responsible for forward particle production can be obtained from the study of particle correla-

tions. In particular, strong azimuthal correlations of hadron pairs are expected when particle production arises from $2 \rightarrow 2$ parton scattering.

This paper reports cross sections for forward inclusive π^0 production for p+p collisions at $\sqrt{s}=200$ GeV. The azimuthal correlations between a forward π^0 ($\langle \eta_\pi \rangle = 4.0$) and mid-rapidity charged hadrons were studied. In addition, exploratory studies with d+Au collisions at $\sqrt{s_{NN}}=200$ GeV are reported, and azimuthal correlations of hadron pairs are compared to those for p+p collisions. The inclusive yields of π^0 mesons in p+p and d+Au collisions will be forthcoming, and details pertinent to this analysis are presented here. Forward π^0 production in d+Au collisions refers to observation of the π^0 in the direction of the incident deuteron.

2. EXPERIMENT

The Solenoidal Tracker At RHIC (STAR) is a multipurpose detector at Brookhaven National Laboratory. One of its principal components is a time projection chamber used for tracking charged particles produced at $|\eta| < 1.2$. A forward π^0 detector (FPD) comprising 7×7 matrices of $3.8 \times 3.8 \times 45$ cm³ Pb-glass detectors (towers) was installed ≈ 800 cm from the interaction region near the beam pipe to detect high energy π^0 mesons with $3.3 < \eta < 4.1$. Data were collected over two years of RHIC operations. In the 2002 run, p+p collisions were studied with a pro-

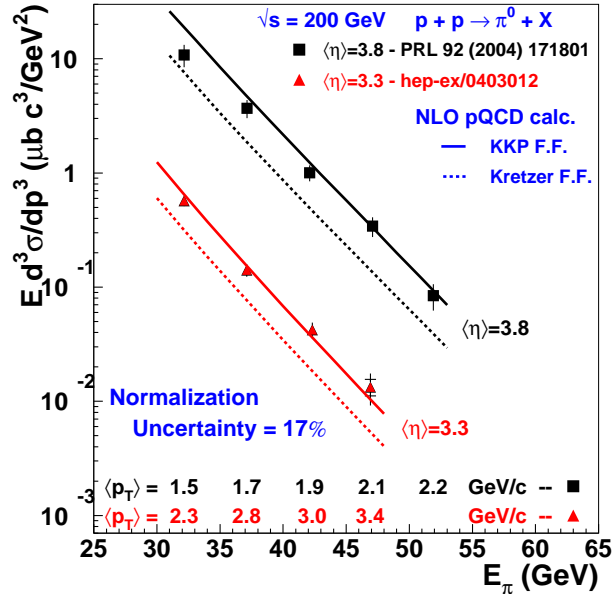


Figure 1. Inclusive π^0 production cross section versus π^0 energy (E_π) at average pseudorapidities ($\langle\eta\rangle$) 3.3 and 3.8. The inner error bars are statistical, and are smaller than the symbols for most points. The outer errors combine these with E_π -dependent systematic errors. The curves are NLO pQCD calculations evaluated at $\eta = 3.3$ and 3.8 using different fragmentation functions.

totype FPD [8]. In the 2003 run, p+p collisions were studied and exploratory measurements were performed with d+Au collisions.

3. DIFFERENTIAL CROSS SECTION

The differential cross section for inclusive π^0 production for $30 < E_\pi < 55$ GeV at $\langle\eta\rangle = 3.8$ was previously reported [8]. The event reconstruction and normalization methods were extended to allow measurement of the differential cross section at $\langle\eta\rangle = 3.3$ [9]. The results are shown in Fig. 1 in comparison to NLO pQCD calculations evaluated at $\eta=3.3$ and 3.8. The NLO pQCD calculations are consistent with the data, in contrast to π^0 data at lower \sqrt{s} [10]. The inclu-

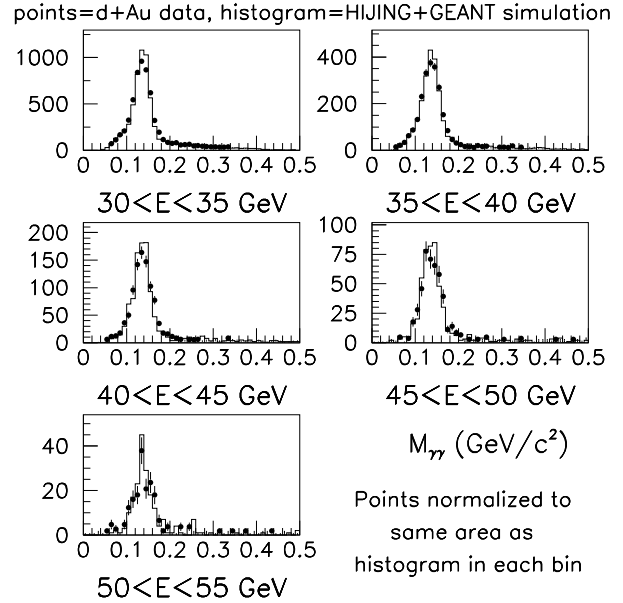


Figure 2. Diphoton invariant mass spectra as a function of energy deposited in the calorimeter for d+Au data and HIJING+GEANT simulations. The histograms are reconstructed simulation events. The points are data with statistical errors, normalized to equal area in each bin.

sive yield was also found to agree with predictions of the PYTHIA event generator [11], which uses initial- and final-state parton showers to model effects beyond leading order.

Nuclear effects on particle production are quantified by R_{dAu} , the ratio of the inclusive yield of particles produced in d+Au collisions to p+p collisions. The value of R_{dAu} for forward π^0 mesons is expected to be smaller than was seen for negative hadrons [1] due to isospin suppression of the $p + p \rightarrow h^- + X$ process [12]. We proceed to discuss considerations relevant to an accurate determination of R_{dAu} for forward π^0 production.

The data in Fig. 1 show that the cross section falls rapidly with E_π . Accurate yield determinations require accurate energy calibrations and good energy resolution. The energy calibration of the FPD is performed by reconstruction of the

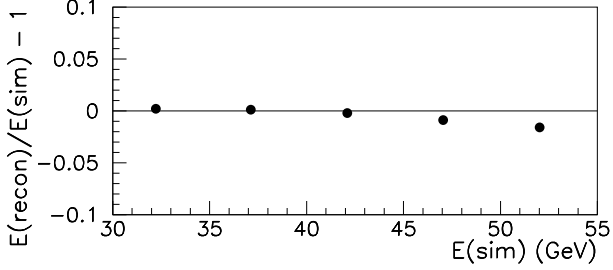


Figure 3. Simulation study of the fractional difference of reconstructed and simulated energy versus simulated π^0 energy. The energy calibration is determined to an accuracy of $\approx 1\%$. Systematics of reconstructing the di-photon opening angle are seen beginning around 50 GeV.

invariant mass of the π^0 meson, $M_{\gamma\gamma}$. An analysis of the topology of the energy deposition, based on measured shower shapes [13], is used to reconstruct the relative energy of the two photons and their separation ($d_{\gamma\gamma}$). The π^0 energy is taken to be the total energy in the calorimeter. The gain of each tower is determined iteratively by associating $M_{\gamma\gamma}$ with the tower containing the most energy in the event. After convergence, an energy-dependent correction is applied to account for material between the interaction region and the detector, which causes decay photons to shower prior to reaching the FPD. It also corrects for the non-linearity implied by using digitizers with a finite number of bits. The energy can be accurately associated with $M_{\gamma\gamma}$ up to a point set by the systematics of reconstructing $d_{\gamma\gamma}$. At 50 GeV, $d_{\gamma\gamma} \approx 1.1 \times$ the linear dimension of a tower. The $M_{\gamma\gamma}$ distribution can be seen in Fig. 2, with resolution $\leq 20 \text{ MeV}/c^2$ from 30 – 55 GeV.

A simulation is used to model the events using the PYTHIA (HIJING)[14] generator for p+p (d+Au) collisions, together with a GEANT simulation to model the detector response, including intervening material. After calibrating the simulation with the same technique as the data, the overlay of data and simulation for $M_{\gamma\gamma}$ can be seen in Fig. 2. The simulation describes the data

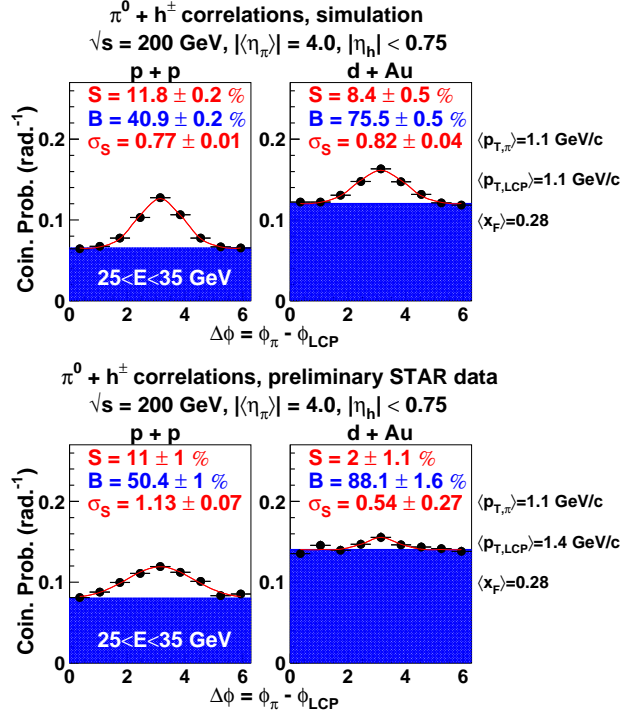


Figure 4. Coincidence probability as function of azimuthal angle difference between a forward π^0 and a midrapidity leading charged particle for p+p (left) and d+Au (right) collisions. The upper plots are simulation using PYTHIA 6.222 and HIJING 1.381 described in the text, while the lower plots are data.

well for $M_{\gamma\gamma}$ as well as several other kinematic variables. The simulations are used to determine the efficiency of π^0 detection. As was observed in [8], the detection efficiency is dominated by the geometrical acceptance of the calorimeter.

Using the simulation, a comparison of the kinematics of events that contain π^0 mesons with reconstructed variables gives an estimate of the accuracy of the analysis techniques used. The fractional difference in energy between the generated and reconstructed π^0 meson in bins of generated π^0 energy can be seen in Fig. 3. The uncertainty on the energy calibration is $\approx 1\%$, implying an

uncertainty on the yield of $\approx 10\%$.

The data in Fig. 1 show that the cross section increases rapidly with η . Accurate yield determinations require accurate position determinations. A Beam Position Monitor (BPM) is located in the vicinity of the FPD, and has been accurately surveyed. Relative to the BPM, the absolute position of the FPD is presently measured with an accuracy of 5 mm, giving an absolute accuracy of $\delta\eta = 0.02$ at $\eta = 4.00$. This implies an uncertainty on the yield of 11%.

4. CORRELATIONS

Correlations between a π^0 produced at large rapidity with large Feynman x and charged particles produced at midrapidity were studied with p+p collisions and d+Au collisions. Details of the analysis, including detailed comparisons to simulations, may be found in Ref. [5]. The leading charged particle (LCP) analysis selects the mid-rapidity track with the highest $p_T > 0.5$ GeV/c, and computes the azimuthal angle difference $\Delta\phi = \phi_{\pi^0} - \phi_{LCP}$ for each event. The normalized $\Delta\phi$ distributions are fit with the sum of a constant and a Gaussian distribution centered at $\Delta\phi = \pi$. The fit parameters are the area under the Gaussian (S), representing the azimuthally correlated coincidence probability; the uncorrelated coincidence probability (B); and the Gaussian width (σ_S). The normalized $\Delta\phi$ distribution for d+Au collisions is shown in comparison to p+p for both simulations and data in Fig. 4. The simulations account for detector resolution and reconstruction efficiency for both the forward π^0 and the midrapidity charged particles.

We observe a large increase of B_{dAu} relative to B_{pp} . The growth in B arises from additional nucleon-nucleon collisions as the deuteron and Au beams interact. For the data, σ_S^{dAu} is much smaller than σ_S^{pp} , most likely reflecting the inadequacy of the functional form used to represent $\Delta\phi_{dAu}$. The azimuthally correlated $\pi^0 + h^\pm$ coincidence probability is smaller in d+Au collisions than in p+p collisions, qualitatively consistent with behavior predicted in a gluon saturation picture [6]. Complete assessment of systematic errors is underway.

5. SUMMARY

In summary, cross sections for the inclusive production of π^0 mesons in p+p collisions at $\sqrt{s}=200$ GeV, at $\langle\eta_\pi\rangle=3.3$ and 3.8 are consistent with NLO pQCD calculations. The azimuthal correlation between pairs of hadrons separated by large $\Delta\eta$ is described by PYTHIA [11], which uses leading order pQCD with parton showers. Agreement of these calculations with the inclusive cross section and di-hadron correlations suggest that forward π^0 production arises from partonic scattering at this collision energy. Exploratory studies of forward π^0 production in d+Au collisions suggest that the azimuthally correlated component of hadron pairs separated by large $\Delta\eta$ is suppressed relative to p+p collisions. More data for forward particle production and di-hadron correlations in d+Au collisions are required to reach a definitive conclusion about the possible existence of gluon saturation in the Au nucleus.

REFERENCES

1. I. Arsene *et al.*, Phys. Rev. Lett. **93** 242303 (2004).
2. D. Kharzeev, Y. V. Kovchegov and K. Tuchin, Phys.Rev. D **68** 094013 (2003).
3. J. Jalilian-Marian, nucl-th/0402080.
4. R. Vogt, hep-ph/0405060.
5. A. Ogawa for the STAR Collaboration, nucl-ex/0408004.
6. D. Kharzeev, E. Levin and L. McLerran, hep-ph/0403271.
7. S.S. Adler *et al.*, Phys. Rev. Lett. **91**, 241803 (2003).
8. J. Adams, *et al.*, Phys. Rev. Lett. **92** 171801 (2004).
9. L.C. Bland for the STAR Collaboration, hep-ex/0403012.
10. C. Bourrely and J. Soffer, Eur. Phys. J. C **36**, 371 (2004).
11. T. Sjöstrand, *et al.*, Comp. Phys. Commun. **135**, 238 (2001).
12. V. Guzey, M. Strikman and W. Vogelsang, Phys. Lett. **B603**, 173 (2004).
13. A. A. Lednev, Nucl. Instrum. Meth. A **366**, 292 (1995).

14. X. N. Wang and M. Gyulassy, Phys. Rev. D **44** 3501 (1991).